H2 excitation in turbulent interstellar clouds

Mon. Not. R. Astron. Soc. **364,** 1309–1314 (2005) doi:10.1111/j.1365-2966.2005.09652.x

H_2 excitation in turbulent interstellar clouds

Cesare Cecchi-Pestellini,[1] Silvia Casu[1]⋆ and Alexander Dalgarno[2]

[1]*INAF – Osservatorio Astronomico di Cagliari, Strada n.54, Loc. Poggio dei Pini, 09012 Capoterra (CA), Italy*
[2]*Harvard–Smithsonian Center for Astrophysics, 60 Garden Street, Cambridge, MA 02138, USA*

Accepted 2005 September 27. Received 2005 September 27; in original form 2005 June 14

ABSTRACT

We discuss the observational differences between lines of sight that intercept a group of turbulent dissipative structures and lines of sight that cross less-active regions. Using time-dependent calculations we show that the energy level distribution of the hydrogen molecule evolves in time in response to the local thermal phase. We find that relatively simple models can explain the observed properties of molecular hydrogen in diffuse interstellar clouds in terms of time evolution induced by collisional excitation in a low-density, high-temperature gas.

Key words: molecular processes – turbulence – ISM: clouds – ISM: molecules.

1 INTRODUCTION

Diffuse interstellar clouds have been extensively studied both observationally and theoretically in the past several decades (Black & Dalgarno 1977; van Dishoeck & Black 1986; Spaans 1996; Kopp, Roueff & Pineau de Forêts 2000; Zsargó & Federman 2003; Le Petít, Roueff & Herbst 2004). Diffuse clouds are generally illuminated by the average diffuse interstellar radiation field, and their chemistry and thermodynamics are directly linked to the radiation and gas densities. As such, these regions were expected to be ideal environments for the understanding of ion–molecule chemistry in interstellar space as well as the physical structure of the galactic interstellar medium (ISM).

Despite their apparent simplicity, the actual nature of diffuse interstellar clouds is elusive. Recent millimetre observations (Lucas & Liszt 2000; Liszt & Lucas 2001; Lucas & Liszt 2002; Liszt & Lucas 2002; Liszt Lucas & Black 2004) have shown that complex molecules may achieve dark-cloud abundances in diffuse interstellar clouds, suggesting the existence of a rich chemistry even at low-visual extinctions. Models of quiescent diffuse cloud chemistry may possibly succeed in explaining the abundance distribution of OH, CN, C_2 and CH, but fail in reproducing the CO, CH^+, HCO^+, H_3^+ column densities. As noted by Liszt & Lucas (2000), if the observed relatively constant abundance of HCO^+ is inserted into the standard chemical models of diffuse clouds undergoing the (H–H_2) transition, the observed variation of the CO column density can be explained without resorting to any other assumption. Moreover, equilibrium excitation analyses provide evidence that a large amount of CH originates from CH^+ chemistry (Zsargó & Federman 2003). Failures and inconsistencies seem thus related to the understanding of the reaction pathways to HCO^+ and CH^+, which require energy sources in excess of the average energy density of diffuse and translucent clouds. The basic problem for the chemistry is how to incorporate the ambient oxygen and carbon into molecules. Oxygen is ionized by slow charge transfers with H^+, while the abundant ionized carbon does not react rapidly with H_2. Most theoretical models rely on the endothermic reactions $C^+ + H_2 \rightarrow CH^+ + H$ ($\Delta E/\kappa \sim 5000$ K) and $O + H_2 \rightarrow OH + H$ ($\Delta E/\kappa \sim 3000$ K). The need for hot chemistry has given rise to consideration of models involving shocks (Flower & Pineau de Forêts 1998) and trapping of low-density gas in a vortex, representative of local dissipation of turbulence (Falgarone, Pineau de Forêts & Roueff 1995; Joulain et al. 1998).

Many observational facts, such as line width–size relations, the large Reynolds numbers of the gas motions and cloud clumping, are consistent with the existence of turbulence within interstellar clouds (cf. Elmegreen & Scalo 2004, and reference therein). Specific signatures of turbulence in interstellar clouds have been searched for, and, starting from the same data, different models have been developed (Elmegreen & Falgarone 1996; McKee & Holliman 1999; Curry & McKee 2000). In particular, Falgarone et al. (1994) noted the similarity between observed molecular line shapes and spectra synthesized from a simulated turbulent velocity and raised the possibility that linewings in non-star-forming clouds trace the intermittency of the velocity field. Miesch & Scalo (1995) performed a similar analysis in star-forming regions.

Analysing maps of ^{12}CO and ^{13}CO lines around low-mass starless dense cores, Pety & Falgarone (2003) inferred that the probability distribution functions of centroid velocity increments have non-Gaussian wings which are the most prominent for the smallest lag. Furthermore, the locations on the maps populating the non-Gaussian wings of the velocity gradients are not randomly distributed, forming small-scale elongated structures. In analogy with the behaviour of such probability distribution functions in laboratory flows or numerical simulations, Pety & Falgarone (2003) proposed that these regions might trace locations of enhanced dissipation in interstellar turbulence. In this picture, the cold diffuse ISM contains pockets of

⋆E-mail: silvia@galileo.dsf.unica.it

hot gas, originating from localized dissipation of non-thermal energy of supersonic turbulence concentrated in shocks and in regions of large shear at the boundary of coherent vortices. Joulain et al. (1998) studied the chemistry of low-density gas trapped in a vortex: chemical evolution is localized within very small regions ($L_\mathrm{v} \lesssim$ 50 au) of low density ($n_\mathrm{H} \sim 30\,\mathrm{cm}^{-3}$) and short lifetimes (a few 100 yr), and it is driven by a sharp increase in the temperature. A large number of such vortices ($\mathcal{N}_\mathrm{v} \sim 1\,000$) must be intercepted at any time along a line of sight to reproduce the observed column densities, but the column density associated with the total aggregate length of the hot gas is only a few per cent of the total column density along the line of sight.

It is implicit in such a process that the excitation state of molecular and atomic gas must change with time in response to the local thermal phase. This paper proposes that the energy level distribution of the main molecular component in the ISM, H_2, evolves in time along turbulent lines of sight. We illustrate this behaviour in a study that explores the changing nature of the excitation properties in turbulent dissipative structures compared to the standard excitation of cold gas in diffuse interstellar clouds. Recent observations (Gry et al. 2002; Falgarone et al. 2005) directly probe the existence of such warm H_2 in the cold diffuse medium.

In Section 2, we describe in detail the model and the procedures we have followed. In Section 3, we discuss possible observational implications. The conclusions are summarized in Section 4.

2 H_2 LEVEL POPULATIONS

The space–time intermittent distribution of the dissipation rate of kinetic energy in turbulent interstellar clouds generates transient and localized hot regions embedded in cooler gas (Falgarone et al. 1995). According to Joulain et al. (1998), the thermal inertia of the medium is such that typical energy-injection times of approximately 100 yr are needed for the gas to reach a temperature maximum T_h. After having experienced an energy-injection burst, the time during which the fluid-cell temperature is raised to values close to T_h is estimated to be $\Delta t_\mathrm{h} \sim 200$ yr (Joulain et al. 1998).

One major effect of turbulent kinetic energy dissipation is the departure from chemical and thermal equilibrium of the gas trapped in the vortex. We have constructed models to compute the H_2 level distribution expected in diffuse interstellar regions subject to localized high-temperature transients. We follow the departure from statistical equilibrium and the evolution in time of the energy level system of H_2 embedded in a perturbed fluid cell. The $\mathcal{M}$ populations n_i ($i = v, J$) of the excited H_2 levels are solutions to the set of stiff differential equations

$$\frac{\mathrm{d}n_i}{\mathrm{d}t} = \sum_{j\neq i} n_j \left(A_{ji} + C_{ji} + W_{ji}\right) - n_i \times \left\{\sum_{j\neq i}(A_{ij} + C_{ij} + W_{ij}) + \beta_i + \zeta + \mathcal{D}\right\} + \mathcal{R} n_\mathrm{H} n_1 \delta_i . \quad (1)$$

The excitation of ro-vibrational levels results from H_2 formation pumping, ultraviolet (UV) absorption of diffuse starlight in the electronic transitions to the excited states B, C, B', and D followed by fluorescence, quadrupole cascading and collisional excitation and de-excitation. In equation (1) W_{ij} are the excitation rates from the level i to level j via UV pumping, A_{ij} are the Einstein coefficients for spontaneous radiative decay, C_{ij} are the temperature-dependent collisional rates, and β_i is the rate of photodissociation out of the level i. The cosmic-ray destruction rate is denoted by ζ, and $\mathcal{D}$ is the rate of additional destruction processes, such as collisional dissociation and ionization. The last term on the right-hand side of equation(1) describes the formation of H_2 via grain catalysis: δ_i is the fraction of H_2 formed on grain surfaces that leaves the grain in level i and n_1 is the concentration of atomic hydrogen. We use a standard formation rate $\mathcal{R} = 3 \times 10^{-17}\,\mathrm{cm}^3\,\mathrm{s}^{-1}$ (Jura 1975), and the model proposed by Black & Dalgarno (1976) for formation pumping. We describe the depth-dependent H_2 photodissociation rates by self-shielding functions (van Dishoeck & Black 1988; Sternberg & Dalgarno 1995), including the prescription for line overlap given in Draine & Bertoldi (1996). All radiation-induced processes have been computed taking into account dust extinction which we assume is described by the mean galactic interstellar extinction curve. We consider a plane-parallel model cloud of constant density and kinetic temperature. The cloud is single-side illuminated by a normally incident UV radiation field (Draine 1978). We include $\mathcal{M} = 300$ bound states of H_2, with $J \leqslant 30$. The highest-lying state is $v, J = (3, 27)$ at about 52 000 K above the ground state. The level populations are subject to the normalization condition $n_\mathrm{H} = n_1 + 2n_2$ where $n_2 = \sum_i n_i$ is the H_2 volume density.

We include inelastic collisions with H, He, and ortho and para H_2, with fully quantum mechanical calculations of collisional rates given in Flower, Roeuff & Zeippen (1998), Flower & Roueff (1998) and Le Bourlot, Pineau des Forêts & Flower (1999). For levels where quantum calculations are not available we adopt the (tentative) extrapolation scheme for the H–H_2 rate collisions proposed by Le Bourlot and co-workers in their PDR code (Le Bourlot, private communication). For all other collisional partners when quantum calculations are lacking we adopt the prescription given in Tiné et al. (1997). The rate coefficients for pure rotational transitions in the ground vibrational state through H^+–H_2 collisions are taken from Gerlich (1990). Energy levels, transition and dissociation probabilities for electronic transitions have been published by Abgrall et al. (1992, 1993a,b) and Abgrall, Roueff & Drira (2000). We use data kindly provided by Abgrall (private communication), covering levels up to $J = 25$. Quadrupole radiative decays and energies of ro-vibrational levels of the ground electronic state were taken from Wolniewicz, Simbotin & Dalgarno (1998).

The non-equilibrium models we present in this work are calculated using as initial conditions the results of statistical equilibrium calculations at gas temperatures ($T_\mathrm{c} = 50$–$200\,\mathrm{K}$) and densities ($n_\mathrm{H} \lesssim 100\,\mathrm{cm}^{-3}$) characteristic of the diffuse ISM (Shull et al. 2000; McCall et al. 2002; Sonnentrucker et al. 2002). We use a step function in temperature to describe the thermal history of a gas pocket trapped in a vortex, that is, we neglect both the energy injection and the cooling phases. A parcel of gas of density n_H located inside a cloud at a visual extinction A_V (mag) from the edge, and with initial kinetic temperature T_c is suddenly heated to a temperature characteristic of those turbulent dissipation events which are neither the most powerful (the rarest) nor the weakest, that is, $T_\mathrm{h} = 1000$–2000 K (Joulain et al. 1998). After a high-temperature phase of duration Δt_h, the gas kinetic temperature drops to the initial value T_c. We do not include the effects of repeated impulsive heatings.

The system in equation (1) is integrated for a time equal to Δt_h, during which the gas kinetic temperature is T_h. After the drop of gas temperature back to the initial value T_c at $t = \Delta t_\mathrm{h}$, we let the H_2 energy level system relax to a steady-state distribution. In Figs 1(a) and (b) is shown the time evolution of the first five energy levels ($v = 0$, $J = 0$–4) in two particular cases representative of the results obtained by numerical simulations. During the high-temperature phase, the populations of pure rotational levels $J = 0$ and 1 decrease while the populations of higher-energy states increase in response

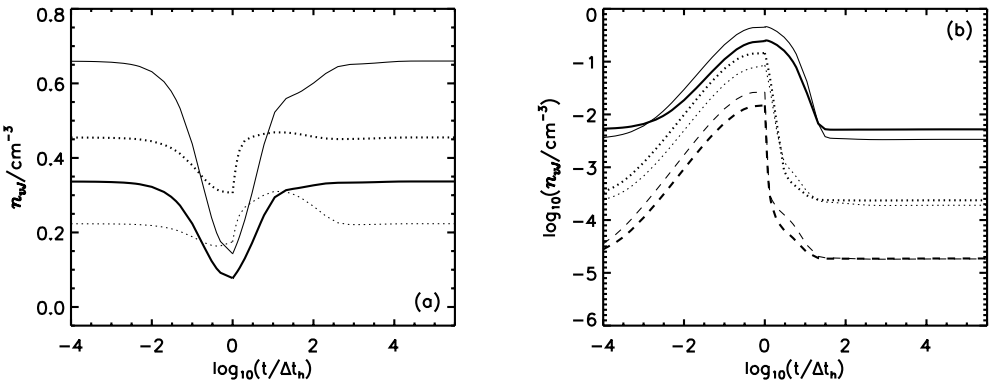

Figure 1. Time evolution of the first five energy levels of H_2 in its ground vibrational state. (a) Solid line $J = 0$; dotted line $J = 1$. (b) Solid line $J = 2$; dotted line $J = 3$; dashed line $J = 4$. The gas density is $n_H = 30\,cm^{-3}$, and the temperature of the hot phase is $T_h = 1\,500$ K. Hot gas pockets are located at $A_V = 0.1$ mag. Thick lines: $T_c = 100$ K; thin lines: $T_c = 50$ K. Times are referred to the duration of the high-temperature phase $\Delta t_h = 200$ yr.

to the new physical conditions. After the fall of temperature back to T_c, the populations of the first two rotational states return to their initial values, following evolutionary paths that depend on the details of the model boundary conditions. In any case, the time-scale of the onset of statistical equilibrium at T_c is considerably longer than Δt_h (Fig. 1a). During the process higher-energy levels follow strictly the rise and the fall of gas kinetic temperature (Fig. 1b), while the volume density of H_2, n_2, does not show significant departures from the unperturbed value.

H_2 trapped in a vortex never reaches equilibrium during the high-temperature phase because the lifetimes of coherent vortex filaments are much shorter than the slow-relaxation time of the lowest-lying levels of H_2. In Fig. 2, we show the time evolution of H_2 volume density and the first five energy levels ($v = 0$, $J = 0$–4) allowing complete relaxation to steady state at the temperature T_h, that is, setting $\Delta t_h \to \infty$. About few 100 yr after the temperature rise, energy level populations reach an unstable equilibrium (Figs 2c and e) which lasts for about 10^4–10^5 yr. At later times, level populations, and thus the H_2 volume density (Fig. 2a), decrease in response to an increased photodestruction rate. The effect is due to the opening of a larger number of destruction channels and to larger photodissociation rates from excited ro-vibrational states. Then, using as initial conditions the steady-state level distribution at T_h, the system (1) is integrated until equilibrium at temperature T_c is again reached. The time evolution in the cold gas is shown in Figs 2(b), (d) and (f): the populations of the energy levels are out of equilibrium for a time approximately 10^5–10^6 yr, before regaining their steady-state values at T_c. The evolution of both hydrogen volume density and energy level system are radically different from those illustrated in Fig. 1: in that case ($\Delta t_h = 200$ yr) the excitation plateau experienced by molecular energy levels during continuous heating ($\Delta t_h \to \infty$) and the drop in volume numerical density of H_2 are absent.

When the intermittent nature of the turbulent energy injection is implemented in the modelling procedure (Fig. 1), the net result is that of a *thermally excited hydrogen gas with a volume density characteristic of cold regions*. The energy level populations show large departures from their stationary values in a cool gas as a result of collisional pumping.

Even if the hot gas fills a very small fraction of the cloud volume, the aggregate column density of H_2 excited levels in dissipative structures along the line of sight might give rise to observable effects. Thus, both the UV absorption spectrum and the infrared (IR) emission of H_2 appear to be suitable probes of dissipative structures induced by interstellar turbulence in diffuse interstellar regions. If a line of sight crosses a region of such kinetic energy dissipation, both hot and cold gas contribute to the H_2 observed level distribution, reflecting the response of the hydrogen molecule to such extreme physical conditions.

3 OBSERVATIONAL IMPLICATIONS

In the preceding section we have shown that the energy level distribution of the hydrogen molecule evolves in time in response to the intermittent dissipation of turbulent kinetic energy.

In Fig. 3, we present H_2 rotational excitation diagrams constructed with level column densities $N_i(i = v, J)$ as functions of excitation energy $\Delta E(v, J)$. Column densities are weighted with the factor $g_i = g_N\,(2J + 1)$, where g_N is the nuclear spin weight that has value $g_N = 1$ for even values of the rotational quantum number J and $g_N = 3$ for odd values of J. We assume the cloud total hydrogen column density to be $N_H = 2 \times 10^{21}\,cm^{-2}$, corresponding to a visual extinction $A_V = 1$ mag, a hydrogen volume density $n_H = 30\,cm^{-3}$ and two values for the temperature of the cold gas, $T_c = 50$ (Fig. 3a) and 100 K (Fig. 3b). The aggregate size pertaining to dissipative structures is taken to be $\Delta L^* = 50\,000$ au, corresponding to roughly 1000 vortices and to a total hydrogen column density $N_H^* \sim 0.01 N_H$. The hot gas has a temperature $T_h = 1500$ K.

We show separately the contribution to the level column densities of both cold H_2 [in equilibrium: stationary solutions to equation (1) at T_c], and hot H_2 [out of equilibrium: solutions to equation (1) at the end of the high-temperature phase $t = \Delta t_h$]. In the figure are also reported the excitation temperatures derived from a fit to the computed column densities of rotational levels $J = 3$–5 of the ground vibrational state. The values found, $T_{ex} \gtrsim 300$ K, depend on the details of the models explored.

Recently, Gry et al. (2002) analysed far-UV absorption spectra obtained with the *Far Ultraviolet Spectroscopic Explorer* (*FUSE*) towards three late B stars to study the formation and excitation of H_2 in the diffuse ISM. Subsequently, Falgarone et al. (2005) presented observations of five pure rotational lines of H_2 obtained with the Short Wavelength Spectrometer (SWS) aboard the *Infrared Space Observatory* (*ISO*) along a line of sight through the Galaxy which avoids regions of massive star formation. The general result of both *FUSE* and SWS-*ISO* analyses is that the fraction of H_2 column density in excited levels with $J > 2$ cannot be accounted for by the UV pumping of H_2 in a cold gas. Our calculations confirm the findings of Falgarone et al. (2005): turbulent hot regions of small linear filling factor provide such excitation temperatures together

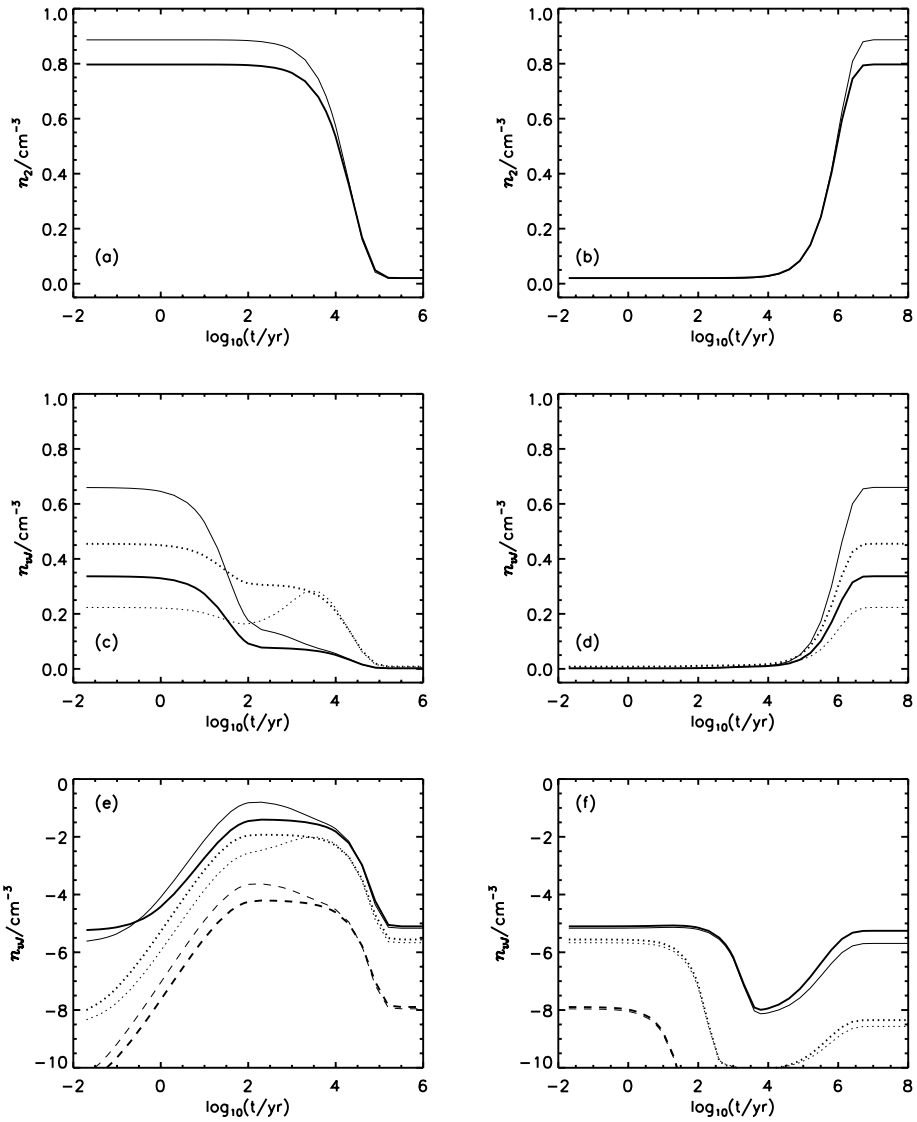

Figure 2. Time evolution of the first five energy levels of H_2 in its ground vibrational state. The physical conditions of the cold gas are as in Fig. 1. H_2 volume density: (a) and (b). Levels $J = 0$ (solid line) and $J = 1$ (dotted line): (c) and (d). Levels $J = 2$ (solid line), $J = 3$ (dotted line), and $J = 4$ (dashed line): (e) and (f).

with large amounts of excited warm H_2 in an otherwise cold diffuse cloud.

In thermally excited clouds, the gas kinetic temperature needs to be at least equal to the H_2 excitation temperature derived from the $J = 3$–5 levels. However, the derived excitation temperatures cannot be gas kinetic temperatures since the densities in the diffuse medium are not high enough to thermalize levels above v, $J = (0, 1)$. In a cold gas, fluorescence cascade following H_2 UV pumping produces large excitation temperatures but very modest abundances of $J =$ 3–5 levels as clearly shown in Fig. 3. Moreover, Falgarone et al. (2005) show that their SWS-*ISO* observations are also inconsistent with the results of a PDR model of the line of sight. Thus, the two observables $N^*_{J>2} = N^*(0, 3) + N^*(0, 4) + N^*(0, 5)$ and $T_{\rm ex}$, should be understood in terms of turbulent dissipation events. To address this point we present in Fig. 4 a diagram of the expected correlation between $N^*_{J>2}$ and $T_{\rm ex}$ derived from the results of the present numerical simulations, together with the observational results of Gry et al. (2002) and Falgarone et al. (2005).

Quiescent gas results have been derived for gas column densities ranging from $N_{\rm H} = 2 \times 10^{20}$ to 2×10^{21} cm^{-2} ($A_V = 0.1$–1.0 mag), $n_{\rm H} = 30$ and 100 cm^{-3}, and $T_{\rm c} = 50$–200 K. The aggregate size of dissipative structures is $\Delta L^* = 50\,000$ au, corresponding to $N^*_{\rm H} = 2.25 \times 10^{19}$ and 7.5×10^{19} cm^{-2}, for $n_{\rm H} = 30$ and 100 cm^{-3}, respectively. Turbulent spots have been located at $A_V = 0.05$, 0.1, 0.2 and 0.5 mag from the edge of the cloud. The temperatures have been assumed to be $T_{\rm h} = 1000, 1500$ and 2000 K. $N^*_{J>2}$ and $T_{\rm ex}$ appear to be well correlated in the cold gas, and, for fixed temperature of the dissipation events or location inside the cloud, even in the hot gas.

In the cold gas, the largest excitation temperatures are, as expected, obtained in the more transparent clouds. In these environments, the concentration of warm gas is very modest since H_2 is heavily photodissociated. $N^*_{J>2}$ increases and $T_{\rm ex}$ decreases with increasing cloud thickness, as the UV radiation density declines due to H_2 self-shielding and dust extinction. A significant concentration of warm H_2 is produced in cold clouds with $A_V = 1$ mag and

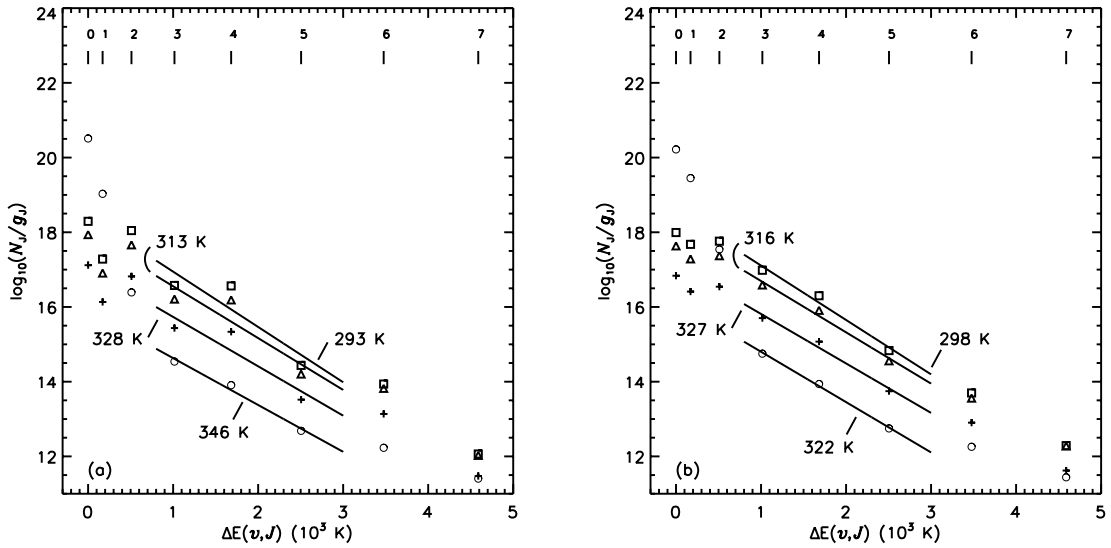

Figure 3. H_2 excitation diagrams. Empty circles represent the contribution of quiescent gas. The hydrogen column densities of cold and hot gas are $N_H = 2 \times 10^{21}$ cm^{-2} and $N_H^* = 7.5 \times 10^{18}$ cm^{-2}, respectively. The hot spots of temperature $T_h = 1\,500$ K are located at $A_V = 0.1$ (crosses), 0.2 (triangles), and 0.5 mag (squares) inside the cloud. (a) $T_c = 50$ K; and (b) $T_c = 100$ K.

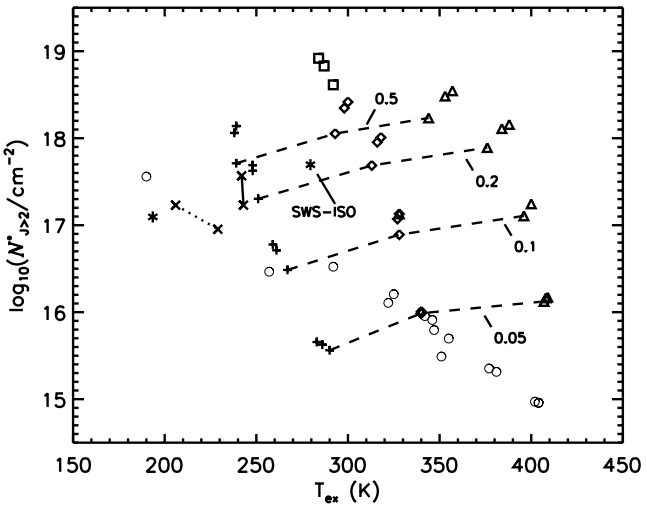

Figure 4. Synthetic $N^*_{J>2}$–T_{ex} correlation. Empty circles: quiescent cold gas; crosses: hot gas $T_h = 1000$ K, $n_H = 30\,\mathrm{cm}^{-3}$; diamonds: hot gas $T_h = 1500$ K, $n_H = 30\,\mathrm{cm}^{-3}$; triangles: hot gas $T_h = 2000$ K, $n_H = 30\,\mathrm{cm}^{-3}$; boxes: hot gas $T_h = 1000$ K, $n_H = 100\,\mathrm{cm}^{-3}$. The filled star labelled as SWS-*ISO* denotes IR observations by Falgarone et al. (2005), while the other star, the solid line and the dotted line refer to absorption measurements of HD 108927, HD 102065 and HD 96675, respectively (Gry et al. 2002). Dashed lines indicate different locations within the cloud: labels refer to visual extinction A_V (mag).

$T_c \gtrsim 150$ K. Although the amount of warm gas can be comparable to that generated in some turbulent models, the excitation temperatures are much lower than those arising in the turbulent gas ($T_{ex} \lesssim 200$ K). Warm H_2 is largely produced in turbulent dissipative spots with the efficiency depending on the location of gas pockets inside the cloud, the temperature and the density of the turbulent layer.

From the results shown in Fig. 4, it appears as follows.

(i) Gas densities $n_H \gtrsim 100\,\mathrm{cm}^{-3}$ and turbulence-induced temperature $T_h \gtrsim 1\,500$ K give rise to excitation temperatures too large with respect to the available observational data;

(ii) *FUSE* observations of the line of sight towards HD 102065 (Gry et al. 2002) are consistent with turbulent spots of temperature $T_h \sim 1\,000$ K, embedded in a layer located approximately at $A_V \gtrsim 0.2$ mag inside a cloud of density $n_H \sim 30\,\mathrm{cm}^{-3}$; hotter gas, $T_h \sim 1\,300$ K, is needed to explain SWS-*ISO* data; and

(iii) along the lines of sight towards HD 108927 and HD 96675 (Gry et al. 2002) the gas seems to intercept only marginally turbulent active regions with the observed concentrations of H_2 in excited rotational states also consistent with UV pumping in a quiescent gas of temperature $T_c \sim 150$ K.

Interestingly, the column density of CH^+, considered an indirect probe of energy release by interstellar turbulence, detected towards HD 96675 is about a factor of 4 smaller than the one observed towards HD 102065.

4 CONCLUSIONS

In diffuse clouds, the low-J lines are typically assumed to provide a measure of the gas temperature while the excitation of the $J > 2$ levels is interpreted as a result of the fluorescent cascade following UV pumping of cold H_2. Recently, by means of *FUSE* spectra towards three late B stars (Gry et al. 2002) and SWS-*ISO* data (Falgarone et al. 2005) these assumptions have been questioned. These observations suggest that the H_2 excitation in the $J > 2$ levels is the result of collisional excitation in regions where the gas is much warmer than usually assumed in the cold diffuse ISM.

In this work, we have presented computational models of turbulent diffuse H_2 clouds, and we compared the results of those models to the available observations. Although we have not attempted to provide precise fits to the observed interstellar H_2 level column densities along particular lines of sight, we have shown that relatively simple models can explain the observed properties of H_2 in diffuse interstellar clouds in terms of small regions of localized dissipation of turbulence. We find that a very small amount of warm gas, $N_H^* \lesssim 2 \times 10^{19}$ cm^{-2}, is needed to reproduce the observed concentrations of rotational excited ($J > 2$) H_2. This is in agreement with the results of Falgarone et al. (2005) that showed that the observed line

intensities are consistent with the line emission of a large number of magnetohydrodynamics (MHD) shocks or magnetized coherent vortices dispersed along the line of sight. We also find that, in dissipative structures, warm H_2 abundances correlate remarkably well with excitation temperatures derived from the $J = 3$–5 levels.

The existence of hot gas in the diffuse ISM has been considered along many lines of sight to account for the observed abundances of CH^+. Formation of CH^+ can be quantitatively investigated including in the chemical modelling procedure localized volumes of hot gas created and sustained by dissipation of gas kinetic energy, as within MHD shocks (Flower & Pineau de Forêts 1998) or coherent small-scale vortices in MHD turbulence (Joulain et al. 1998). It is very difficult on the basis of the abundances they produce, to distinguish between a few MHD shocks or a much larger number of small vortices distributed within the cold neutral medium, so that the nature of chemically active structures in the diffuse medium has yet to be established. The main differences between MHD shocks and dissipative vortices are their thickness and crossing time. Typically, MHD shocks, that have reached steady state, have warm layers of $\sim$0.1 pc thickness and a crossing time of $\sim 10^4$ yr (Falgarone et al. 2005). Vortices threaded by magnetic fields have a size of approximately 50 au and crossing times of a few 100 yr (Joulain et al. 1998). We note that our approach offers the possibility, at least in principle, to discriminate between the two proposed mechanisms in terms of time-dependent excitation conditions of H_2 (cf. Figs 1 and 2).

Finally, we note that the imprint of the heating burst on the populations of the first two levels of H_2 persists for a period of time that, depending on the model assumptions, might be comparable to the lifetime of diffuse interstellar clouds.

ACKNOWLEDGMENTS

We thank our referee, E. Falgarone, for very useful comments that improved the presentation of this paper.

REFERENCES

Abgrall H., Le Bourlot J., Pineau des Forêts G., Roueff E., Flower D. R., Heck L., 1992, A&A, 253, 525
Abgrall H., Roueff E., Drira I., 2000, A&AS, 141, 297
Abgrall H., Roueff E., Launay F., Roncin J. Y., Subtil J. L., 1993a, A&A, 101, 273
Abgrall H., Roueff E., Launay F., Roncin J. Y., Subtil J. L., 1993b, A&A, 101, 323
Black J. H., Dalgarno A., 1976, ApJ, 132, 142
Black J. H., Dalgarno A., 1977, ApJS, 34, 405
Curry C. L., McKee C. F., 2000, ApJ, 528, 734
Draine B. T., 1978, ApJS, 36, 595
Draine B. T., Bertoldi F., 1996, ApJ, 468, 269
Elmegreen B. G., Falgarone E., 1996, ApJ, 471, 816
Elmegreen B. G., Scalo J., 2004, ARA&A, 41, 211
Falgarone E., Lis D. C., Phillips T. G., Pouquet A., Porter D. H., Woodward P. R., 1994, ApJ, 436, 728
Falgarone E., Pineau de Forêts G., Roueff E., 1995, A&A, 300, 870
Falgarone E., Verstraete L., Pineau de Forêts G., Hily-Blant P., 2005, A&A, 433, 997
Flower D. R., Pineau de Forêts G., 1998, MNRAS, 297, 1182
Flower D. R., Roueff E., 1998, J. Phys. B, 31, 2935
Flower D. R., Roueff E., Zeippen C. J., 1998, J. Phys. B, 31, 1105
Gerlich D., 1990, J. Chem. Phys. 92, 2377
Gry C., Boulanger F., Nehmé C., Pineau des Forêts G., Habart E., Falgarone E., 2002, A&A, 391, 675
Joulain K., Falgarone E., Pineau des Forêts G., Flower D. R., 1998, A&A, 340, 241
Jura M., 1975, ApJ, 197, 575
Kopp M., Roueff E., Pineau de Forêts G., 2000, MNRAS, 315, 37
Le Bourlot J., Pineau des Forêts G., Flower D. R., 1999, MNRAS, 305, 802
Le Petít F., Roueff E., Herbst E., 2004, A&A, 417, 993
Liszt H. S., Lucas R., 2000, A&A, 355, 333
Liszt H. S., Lucas R., 2001, A&A, 370, 576
Liszt H. S., Lucas R., 2002, A&A, 391, 693
Liszt H. S., Lucas R., Black J. H., 2004, A&A, 428, 117
Lucas R., Liszt H. S., 2000, A&A, 358, 1069
Lucas R., Liszt H. S., 2002, A&A, 348, 1054
McCall B. J. et al., 2002, ApJ, 567, 391
McKee C. F., Holliman J. H., II, 1999, ApJ, 522, 313
Miesch M. S., Scalo J., 1995, ApJ, 429, 645
Pety J., Falgarone E., 2003, A&A, 412, 417
Shull M. J. et al., 2000, ApJ, 538, L73
Sonnentrucker P., Friedman S. D., Welty D. E., York D. G., Snow T. P., 2002, ApJ, 576, 241
Spaans M., 1996, A&A, 307, 271
Sternberg A., Dalgarno A., 1995, ApJS, 99, 565
Tiné S., Lepp S., Gredel R., Dalgarno A., 1997, ApJ, 481, 282
van Dishoeck E. F., Black J. H., 1986, ApJS, 62, 109
van Dishoeck E. F., Black J. H., 1988, ApJ, 334, 771
Wolniewicz L., Simbotin I., Dalgarno A., 1998, ApJS, 115, 293
Zsargó J., Federman S. R., 2003, ApJ, 589, 319

This paper has been typeset from a TEX/LATEX file prepared by the author.